

A. W. Reske  
A. P. Reske  
H. A. Gast  
M. Seiwerts  
A. Beda  
U. Gottschaldt  
C. Josten  
D. Schreiter  
N. Heller  
H. Wrigge  
M. B. Amato

## Extrapolation from ten sections can make CT-based quantification of lung aeration more practicable

Received: 24 January 2010  
Accepted: 26 April 2010  
Published online: 6 August 2010  
© Copyright jointly held by Springer and ESICM 2010

Preliminary data from this study were presented at the 22nd Annual Congress of the European Society of Intensive Care Medicine in Vienna, October 2009.

A. W. Reske and A. P. Reske contributed equally to this work.

### Electronic supplementary material

The online version of this article (doi:10.1007/s00134-010-2014-2) contains supplementary material, which is available to authorized users.

A. W. Reske (✉) · A. P. Reske · A. Beda  
Department of Anesthesiology and Intensive Care Medicine, University Hospital Carl Gustav Carus, Fetscherstrasse 74, 01307 Dresden, Germany  
e-mail: andreas.reske@uniklinikum-dresden.de  
Tel.: +49-176-14455000  
Fax: +49-341-9405247

H. A. Gast · M. Seiwerts  
Department of Diagnostic and Interventional Radiology, University Hospital Leipzig, Leipzig, Germany

U. Gottschaldt  
Department of Anesthesiology and Intensive Care Medicine, University Hospital Leipzig, Leipzig, Germany

C. Josten  
Department of Trauma and Reconstructive Surgery, University Hospital Leipzig, Leipzig, Germany

D. Schreiter  
Department of Surgery, Surgical Intensive Care Unit, University Hospital Carl Gustav Carus, Dresden, Germany

N. Heller  
Institute of Informatics, University of Leipzig, Leipzig, Germany

H. Wrigge  
Department of Anesthesiology and Intensive Care Medicine, University of Bonn, Bonn, Germany

M. B. Amato  
Pulmonary Division, Cardio-Pulmonary Department, Hospital das Clinicas, University of Sao Paulo, Sao Paulo, Brazil

**Abstract Purpose:** Clinical applications of quantitative computed tomography (qCT) in patients with pulmonary opacifications are hindered by the radiation exposure and by the arduous manual image processing. We hypothesized that extrapolation from only ten thoracic CT sections will provide reliable information on the aeration of the entire lung. **Methods:** CTs of 72 patients with normal and 85 patients with opacified lungs were studied retrospectively. Volumes and masses of the lung and its differently aerated compartments were obtained from all

CT sections. Then only the most cranial and caudal sections and a further eight evenly spaced sections between them were selected. The results from these ten sections were extrapolated to the entire lung. The agreement between both methods was assessed with Bland–Altman plots. **Results:** Median (range) total lung volume and mass were 3,738 (1,311–6,768) ml and 957 (545–3,019) g, the corresponding bias (limits of agreement) were 26 (–42 to 95) ml and 8 (–21 to 38) g, respectively. The median volumes (range) of differently aerated compartments (percentage of total lung volume) were 1 (0–54)% for the nonaerated, 5 (1–44)% for the poorly aerated, 85 (28–98)% for the normally aerated, and 4 (0–48)% for the hyperaerated subvolume. The agreement between the extrapolated results and those from all CT sections was excellent. All bias values were below 1% of the total lung volume or mass, the limits of agreement never exceeded  $\pm 2\%$ . **Conclusion:** The extrapolation method can reduce radiation exposure and shorten the time required for qCT analysis of lung aeration.

**Keywords** Computed tomography · Quantitative imaging · Lung volume measurements · Acute respiratory failure · Pulmonary atelectasis

## Introduction

Quantitative computed tomography-based (qCT) assessment of lung aeration and its alterations (e.g., consolidation or hyperaeration) can help to assess and monitor severity and course of pulmonary disease [1–9], to clarify the etiology and pathophysiology of acute respiratory failure [3, 10–13], to individualize mechanical ventilation [4, 5, 11, 12, 14–16], or to identify patients at risk of developing complications such as ventilator-associated lung injury [3, 5, 11, 16, 17].

The incorporation of such qCT-based information into both research and clinical decision-making is hindered by the inherent radiation exposure as well as by the arduous manual processing of the CT images, which is necessary when automatic segmentation fails because of significant pulmonary opacifications due to atelectasis, consolidation, or edema. Theoretically, both problems could be addressed by obtaining single representative CT sections instead of scanning the entire lung [3, 18–20]. However, previous studies showed that the results obtained from one to three CT sections or combinations thereof did not agree consistently with those read from the entire lung [14, 18–20]. Therefore, despite its drawbacks, quantitative analysis of complete multislice CT of the lung has been advocated and used by several groups [4, 5, 10, 11, 14, 15, 21–23].

In this work, still with the aim of simplifying qCT analysis, we tested the hypothesis that a novel method which requires the analysis of ten CT sections only reliably allows extrapolation of results on lung volume, mass, and size of differently aerated lung compartments to the entire lung.

## Patients and methods

We retrospectively analyzed complete lung CTs performed in emergency patients as part of the diagnostic work-up or in patients with respiratory problems treated in the intensive care unit. The observational analysis of CT data was approved by the institutional ethics committee, which waived the need for informed consent. Further methodological details are provided in the “Electronic supplementary material” (ESM).

### CT analysis

Scanning parameters are given in the ESM. The distribution of pulmonary opacifications was classified according to Puybasset [21]. After manual segmentation of the lung parenchyma, the total lung volume ( $V_{\text{total}}$ ) and mass ( $M_{\text{total}}$ ), the pulmonary gas volume ( $V_{\text{gas}}$ ), and the

volumes and masses of four differently aerated lung compartments were calculated voxel-by-voxel according to established methods [3, 10–12, 15, 24–26].

### Extrapolation

The extrapolation method uses ten CT sections instead of all sections covering the whole lung (all CT sections). The most cranial and caudal CT sections and a further eight evenly spaced CT sections between them were analyzed. In case it was impossible to retrospectively select eight sections at perfectly equal intervals between the most cranial and caudal CT sections, intervals were adapted to obtain an almost even distribution. These ten CT sections were analyzed by using standard segmentation and densitometry methods. The results were extrapolated to the entire lung assuming that the lung volume between two CT sections was approximately conic (Fig. 1) [27, 28].

The procedure was repeated with five and three, respectively, evenly spaced CT sections in 45 patients. To test the accuracy for assessing intraindividual changes, we also analyzed patients for whom additional data from repeat CT were available.

### Statistics

Data are given as median and range (minimum and maximum values) or, if distribution of data was normal, as mean and standard deviation ( $\pm$ SD). The agreement between extrapolated values and the corresponding values calculated from all CT sections was assessed according to Bland and Altman [29, 30]. Bias values were compared with Mann–Whitney or Kruskal–Wallis tests. Bonferroni-corrected Mann–Whitney tests were used for post hoc testing. Statistical significance was assumed at  $P < 0.05$ .

## Results

Further results are provided in the ESM.

We analyzed single CT data sets of 157 patients. The median age of patients was 33 (11–91) years. Thirty-one patients (20%) were female. Thirty-three (21%) patients underwent CT during spontaneous breathing and 124 (79%) during mechanical ventilation. Nine patients (6%) had pneumothoraces.

Seventy-two (46%) patients had a normal lung morphology on CT and 85 (54%) showed pulmonary opacifications. The distribution of opacifications was diffuse in 16 (19%), lobar in 29 (34%), and patchy in 40 (47%) patients.

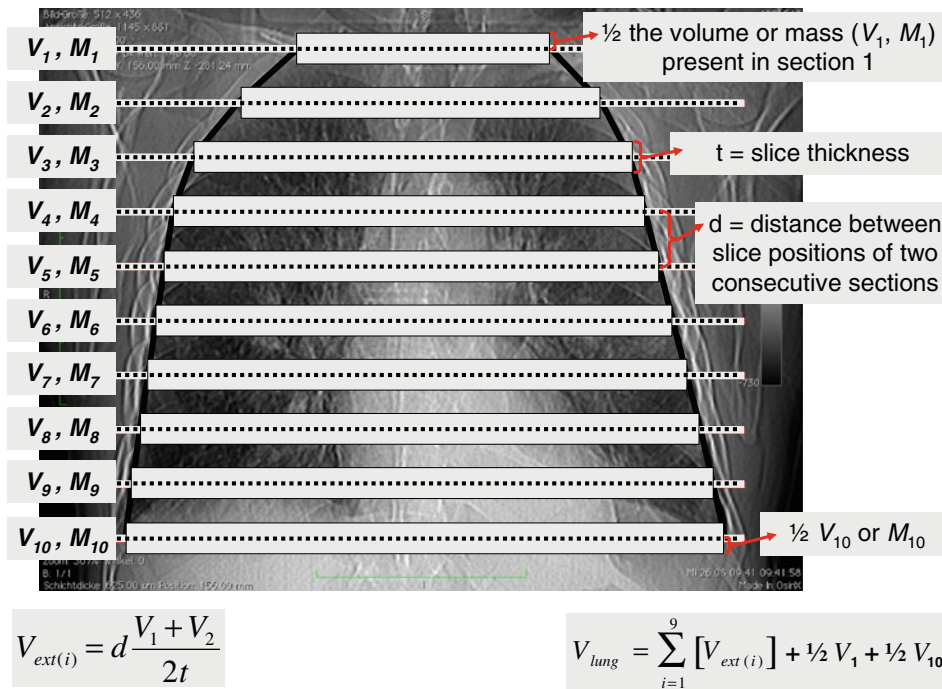


**Fig. 1** Illustrates details of the extrapolation method. *Gray horizontal bars* schematically symbolize CT sections which were selected for extrapolation. The adjustment of the CT sections to lung boundaries (which may seem poor in this schematic illustration) was ensured during segmentation of CT images (see text). *Dotted black lines* refer to the slice position of these CT sections, which can be read from the Digital Imaging and Communication in Medicine (DICOM) header of the respective image. Formulae were adopted from ref. [27]. For

reasons of simplicity, symbols in the formulae (e.g.,  $V_1, V_2$ ) refer only to volume parameters. For the extrapolation of mass parameters, the respective masses (e.g.,  $M_1$ ) are used instead.  $V_{ext(i)}$  denotes the volume or mass in the conic section between two consecutive CT sections (i.e.,  $V_1$  and  $V_2, V_2$  and  $V_3, V_3$  and  $V_4$ , etc.). The volume or mass parameters of the entire lung ( $V_{lung}$ ) are derived from the sum of the nine conic sections and the correction terms ( $\frac{1}{2}V_1$  and  $\frac{1}{2}V_2$ )

Median (range)  $V_{total}$  and  $M_{total}$  calculated from all CT sections were 3,738 (1,311–6,768) ml and 957 (545–3,019) g, respectively. When calculated from all CT sections and expressed as percentage of  $V_{total}$ , the median volumes were 1 (0–54)% for the nonaerated, 5 (1–44)% for poorly aerated, 85 (28–98)% for the normally aerated, and 4 (0–48)% for the hyperaerated compartment. The corresponding masses were 4 (0–79)% for nonaerated, 13 (4–51)% for poorly aerated, 77 (11–94)% for normally aerated, and 1 (0–24)% for hyperaerated. The median  $V_{gas}$  was 2,766 (680–5,379) ml corresponding to 73 (31–87)% of  $V_{total}$ .

Bland–Altman plots for  $V_{total}$  and  $M_{total}$  are given in Fig. 2. For all volume and mass parameters characterizing differently aerated compartments, bias values were below 1% of  $V_{total}$  or  $M_{total}$ , respectively, and the limits of agreement never exceeded  $\pm 2\%$  (Table 1; Fig. 3).

Normal lungs did not have smaller bias values than opacified lungs (all  $P$  values greater than 0.11).

The distribution of opacifications did not significantly influence the agreement of the methods (Table 1).

The bias did not differ between differently aerated lung compartments ( $P = 0.86$ ).

**Fig. 2** Bland–Altman plots of the agreement between the extrapolated value ( $V_{extra}/m_{extra}$ ) and the corresponding value from all CT sections ( $V_{all}/m_{all}$ ) for total lung volume and mass. Data from all lungs analyzed in this study ( $n = 157$ ) were included.  $V_{all}/m_{all}$  mass or volume calculated from all CT sections;  $V_{extra}/m_{extra}$  extrapolated volume or mass; LOA limits of agreement

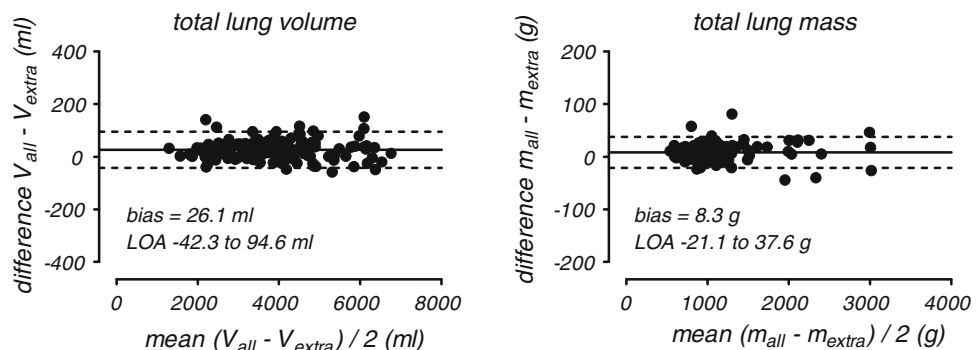


**Table 1** Agreement between extrapolated and corresponding values from all CT sections

	All lungs ( <i>n</i> = 157)	Normal lungs ( <i>n</i> = 72)	Opacified lungs	Diffuse ( <i>n</i> = 16)	Patchy ( <i>n</i> = 40)	Lobar ( <i>n</i> = 29)
			All ( <i>n</i> = 85)			
$V_{total}$ (ml)	26.1 (-42.3 to 94.6)	25.8 (-39.0 to 90.7)	26.4 (-45.4 to 98.1)	15.3 (-48.5 to 78.1)	25.7 (-47.1 to 98.6)	33.4 (-40.5 to 107.3)
$V_{non}$ (%)	0.0 (-0.4 to 0.4)	0.0 (-0.1 to 0.1)	0.0 (-0.6 to 0.5)	0.1 (-0.6 to 0.7)	0.0 (-0.6 to 0.5)	0.0 (-0.6 to 0.5)
$V_{poor}$ (%)*	0.0 (-0.7 to 0.8)	0.0 (-0.5 to 0.6)	0.0 (-0.9 to 0.9)	0.1 (-1.0 to 1.3)	0.0 (-0.9 to 0.9)	-0.2 (-0.7 to 0.4)
$V_{normal}$ (%)*	0.0 (-1.0 to 1.1)	0.0 (-0.9 to 0.9)	0.1 (-1.2 to 1.3)	-0.2 (-1.2 to 0.8)	0.0 (-1.4 to 1.4)	0.2 (-0.6 to 1.1)
$V_{hyper}$ (%)	0.0 (-0.7 to 0.7)	-0.1 (-0.7 to 0.6)	0.0 (-0.7 to 0.7)	0.0 (-0.2 to 0.2)	0.0 (-1.0 to 0.9)	0.0 (-0.5 to 0.5)
$M_{total}$ (g)	8.3 (-21.1 to 37.6)	8.1 (-13.3 to 29.5)	8.4 (-26.5 to 43.2)	15.2 (-17.4 to 47.8)	7.9 (-33.0 to 48.9)	5.1 (-19.1 to 29.4)
$M_{non}$ (%)	0.0 (-1.1 to 1.0)	0.0 (-0.4 to 0.5)	-0.1 (-1.4 to 1.3)	0.0 (-1.1 to 1.2)	-0.1 (-1.7 to 1.4)	0.0 (-1.2 to 1.2)
$M_{poor}$ (%)*	0.0 (-1.2 to 1.3)	0.0 (-1.1 to 1.2)	0.0 (-1.4 to 1.4)	0.2 (-1.2 to 1.6)	0.1 (-1.3 to 1.5)	-0.3 (-1.4 to 0.9)
$M_{normal}$ (%)	0.0 (-1.4 to 1.5)	0.0 (-1.4 to 1.3)	0.1 (-1.5 to 1.6)	-0.2 (-1.3 to 0.9)	0.0 (-1.7 to 1.8)	0.3 (-1.1 to 1.7)
$M_{hyper}$ (%)	0.0 (-0.3 to 0.3)	-0.1 (-0.4 to 0.3)	0.0 (-0.3 to 0.2)	0.0 (-0.1 to 0.1)	0.0 (-0.3 to 0.3)	0.0 (-0.2 to 0.1)
$V_{gas}$ (%)*	0.0 (-0.5 to 0.5)	-0.1 (0.4 to 0.3)	0.0 (-0.6 to 0.6)	-0.1 (-0.5 to 0.3)	0.0 (-0.6 to 0.6)	0.1 (-0.4 to 0.7)

Data are bias and 95% limits of agreement (in parentheses) from the Bland-Altman analysis. Diffuse, patchy, and lobar refer to the subgroups of lungs characterized by different distributions of the opacifications. All subvolumes and submasses were calculated as percentage of  $V_{total}$  or  $M_{total}$ , respectively

$V_{total}/M_{total}$  total lung volume or mass;  $V_{non}/M_{non}$  nonaerated volume or mass;  $V_{poor}/M_{poor}$  poorly aerated volume or mass;  $V_{normal}/M_{normal}$  normally aerated volume or mass;  $V_{hyper}/M_{hyper}$  hyperaerated volume or mass;  $V_{gas}$  pulmonary gas volume

\* Variables for which the omnibus test (Kruskal-Wallis) indicated significant differences between subgroups with different distributions of opacifications. The results of the respective post hoc tests no longer reached statistical significance (Bonferroni-adjusted critical  $P$  value = 0.004)

Images were reconstructed with 5-mm thickness and the standard filter in 46 (29%) and 10-mm thickness and the enhancing filter in 111 (71%) patients. The bias observed in these two groups did not differ for any of the volume or mass parameters analyzed (all  $P$  values greater than 0.15, Table 2).

In a subgroup of 45 patients, the accuracy of the extrapolation method was compared using ten, five, and three CT sections, respectively. These results are given in Table 3 and the ESM.

Intraindividual changes in lung condition occurring between two successive CTs were analyzed in 26 patients. The agreement between the extrapolated changes and the corresponding changes obtained by analysis of all CT sections are shown in Table 4, further results are given in the ESM.

## Discussion

We found an excellent agreement between quantitative descriptors of lung aeration and its alterations extrapolated from ten CT sections and the corresponding values calculated from all CT sections. Our results are of potential importance for qCT analysis of lung aeration because the use of the extrapolation method allows a reduction of radiation exposure and decreases the time required for qCT analysis.

Thoracic qCT is used in patients with acute respiratory failure because it helps in assessing the response to treatment options such as the application of positive end-expiratory pressure (PEEP) [4, 5, 14–17, 22]. In addition, qCT-derived parameters may be markers of disease severity [2, 4, 5, 9]. Despite these potentially useful applications, more frequent use of qCT is, besides problems due to transportation of the patient, currently limited by high radiation exposure and the necessity of arduous manual image processing [3, 11, 26, 31].

Whether or not combined with low-dose CT, prospective use of the extrapolation method (i.e., only ten sections are scanned) can reduce radiation exposure up to several hundred percent [31]. It thus improves the risk-to-benefit balance of qCT and may help to justify research projects. Prospective use of the extrapolation method, however, requires consideration of the technical characteristics of the locally available CT scanner to clarify how scanning can actually be performed (e.g., ten single 5- to 10-mm sections or ten short helical CTs). Moreover, prospective application of the extrapolation method can be limited when the primary indication for CT is the detection of localized lung pathologies.

Our results also appear relevant to the analysis of CT images. In contrast to normal or emphysematous lungs [1, 31, 32], automatic segmentation is challenging in CT images with pulmonary opacifications which are difficult to

**Fig. 3** Bland–Altman plots for the agreement between the extrapolated volume and the volume from all CT sections for the differently aerated lung compartments. Data from all lungs analyzed in this study ( $n = 157$ ) were included. All volumes were calculated as percentage of total lung volume ( $V_{total}$ ).  $V_{all}$  volume calculated from all CT sections;  $V_{extra}$  extrapolated volume;  $LOA$  limits of agreement

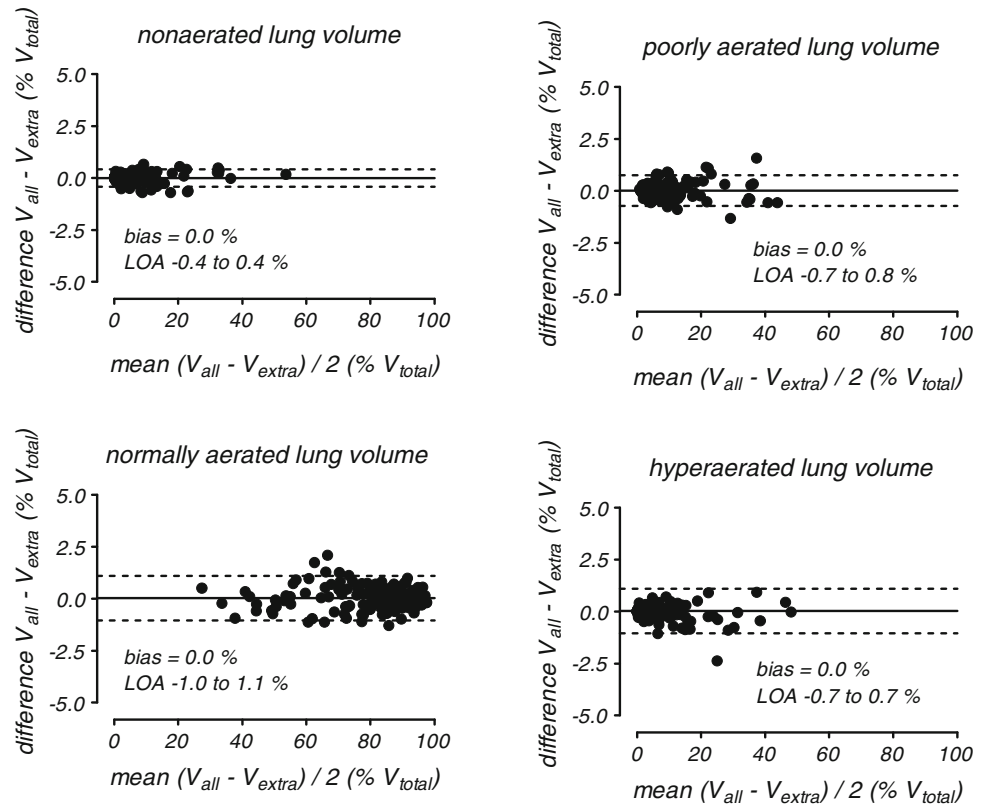


**Table 2** Influence of image reconstruction on the accuracy of extrapolation

	Reconstruction 10 mm B60 <sup>a</sup> ( $n = 111$ )	Reconstruction 5 mm B <sup>b</sup> ( $n = 46$ )
$V_{total}$ (ml)	25.9 (−41.0 to 92.8)	26.7 (−46.1 to 99.5)
$V_{non}$ (%)	0.0 (−0.4 to 0.4)	0.0 (−0.5 to 0.5)
$V_{poor}$ (%)	0.0 (−0.7 to 0.8)	0.0 (−0.7 to 0.7)
$V_{normal}$ (%)	0.0 (−1.0 to 1.1)	0.1 (−1.1 to 1.2)
$V_{hyper}$ (%)	0.0 (−0.7 to 0.7)	−0.1 (−0.7 to 0.6)
$M_{total}$ (g)	7.9 (−19.7 to 35.5)	9.1 (−24.3 to 42.5)
$M_{non}$ (%)	0.0 (−1.1 to 1.0)	0.0 (−1.1 to 1.1)
$M_{poor}$ (%)	0.0 (−1.3 to 1.3)	0.0 (−1.2 to 1.1)
$M_{normal}$ (%)	0.0 (−1.5 to 1.5)	0.0 (−1.4 to 1.4)
$M_{hyper}$ (%)	0.0 (−0.4 to 0.3)	0.0 (−0.3 to 0.2)
Gas content (%)	0.0 (−0.5 to 0.5)	0.0 (−0.5 to 0.5)

Data are bias values (95% limits of agreement) from the Bland–Altman analysis. Statistical testing did not reveal significant differences. All subvolumes and submasses were calculated as percentage of  $V_{total}$  or  $M_{total}$ , respectively

$V_{total}/M_{total}$  total lung volume or mass;  $V_{non}/M_{non}$  nonaerated volume or mass;  $V_{poor}/M_{poor}$  poorly aerated volume or mass;  $V_{normal}/M_{normal}$  normally aerated volume or mass;  $V_{hyper}/M_{hyper}$  hyperaerated volume or mass;  $V_{gas}$  pulmonary gas volume

<sup>a</sup> Refers to CT data sets which were reconstructed with 10-mm slice thickness and an enhancing reconstruction filter

<sup>b</sup> Refers to data sets reconstructed with 5-mm thickness and a standard filter

separate from adjacent thoracic soft tissues or pleural effusions [11, 26, 33–35]. Software developed for automatic segmentation of CT images of pigs with experimental lung injury awaits validation for the use in patients or other research animals [35, 36]. Automatic segmentation using thresholds around −250 HU is also not alternative to the manual processing of images with opacifications because the pathophysiologically most important nonaerated lung compartment with densities between −100 and +100 HU would a priori be excluded from analysis [6, 15, 26, 34]. Therefore, although manual segmentation is highly inefficient, it is often inevitable. The potential for time savings due to the use of the extrapolation method is obvious when considering that the time required for manually processing all images of an average lung CT with 5-mm slice thickness often reaches 6 h.

Pioneering studies in mechanically ventilated patients followed two different principal approaches to reduce the number of CT sections for the analysis of lung aeration. One was to waive the analysis of the entire lung and analyze regional changes instead, which were read from single CT sections positioned at anatomically distinct lung regions, e.g., 2 cm above the dome of the diaphragm [18–20, 37–39]. However,  $V_{total}$ ,  $V_{gas}$ , or  $M_{total}$  cannot be estimated this way and the accuracy of the regional estimates of the size of differently aerated regional lung compartments is highly

**Table 3** Accuracy of extrapolation from different numbers of CT sections

	3 CT sections ( <i>n</i> = 45)	5 CT sections (same patients)	10 CT sections (same patients)
$V_{\text{total}}$ (ml)	920.3 (−10.5 to 1851.1)	54.6 (−250.9 to 360.1)*	24.4 (−38.8 to 87.5)*
$V_{\text{non}}$ (%)	−0.1 (−4.9 to 4.8)	0.3 (−1.5 to 2.0)	0.0 (−0.4 to 0.5)
$V_{\text{poor}}$ (%)	−0.4 (−5.4 to 4.6)	0.2 (−3.0 to 3.5)	0.1 (−0.9 to 1.1)
$V_{\text{normal}}$ (%)	−0.4 (−7.4 to 8.2)	0.1 (−5.0 to 4.8)	−0.1 (−1.3 to 1.1)
$V_{\text{hyper}}$ (%)	0.1 (−3.5 to 3.7)	−0.1 (−2.9 to 2.7)	0.0 (−0.6 to 0.6)
$M_{\text{total}}$ (g)	289.8 (−62.8 to 642.4)	20.9 (−73.7 to 115.5)*	9.8 (−22.4 to 42.0)*
$M_{\text{non}}$ (%)	0.4 (−8.6 to 9.4)	0.1 (−3.5 to 3.7)	0.1 (−1.2 to 1.3)
$M_{\text{poor}}$ (%)	−0.5 (−6.8 to 5.9)	0.2 (−3.5 to 4.0)	0.1 (−1.4 to 1.6)
$M_{\text{normal}}$ (%)	0.2 (−9.5 to 10.0)	−0.2 (−5.2 to 4.9)	−0.2 (−1.8 to 1.4)
$M_{\text{hyper}}$ (%)	−0.2 (−2.7 to 2.3)	−0.1 (−1.8 to 1.6)	0.0 (−0.2 to 0.2)
Gas content (%)	0.2 (−5.1 to 5.6)	−0.1 (−3.1 to 2.9)	−0.1 (−0.6 to 0.5)

Accuracy of the extrapolation method was tested for different numbers of evenly spaced CT sections in the same 45 patients. Data are bias values (95% limits of agreement) from the Bland–Altman analysis. All subvolumes and submasses were calculated as percentage of  $V_{\text{total}}$  or  $M_{\text{total}}$ , respectively

$V_{\text{total}}/M_{\text{total}}$  total lung volume or mass;  $V_{\text{non}}/M_{\text{non}}$  nonaerated volume or mass,  $V_{\text{poor}}/M_{\text{poor}}$  poorly aerated volume or mass;  $V_{\text{normal}}/M_{\text{normal}}$  normally aerated volume or mass;  $V_{\text{hyper}}/M_{\text{hyper}}$  hyperaerated volume or mass;  $V_{\text{gas}}$  pulmonary gas volume

\* $P < 0.0001$  for comparison with “3 CT sections”. Statistical testing did not reveal significant differences between bias values for extrapolation from 5 or 10 CT sections, respectively. Differences between bias values observed for relative subvolumes and submasses or gas content were not statistically significant

variable [11, 14, 18–20, 37]. An approach to obtain information on the entire lung was to use an averaged lung density from single apical, hilar, and juxtadiaphragmatic CT sections and to multiply it by either the gas volume of the lung measured by the helium dilution technique [40], or by the distance between the CT sections [41].

A significant advantage of the extrapolation method is the availability of mass and volume parameters characterizing both the entire lung ( $V_{\text{total}}$ ,  $M_{\text{total}}$ , and  $V_{\text{gas}}$ ) and the differently aerated lung compartments. Our results suggest that extrapolation can be performed with excellent accuracy. Considering the magnitude reported for the interobserver variation of manual segmentation (around 2%) [4, 24, 25, 42] and the fact that deviations smaller than 2% are not considered clinically relevant [32, 43], the accuracy of the extrapolation method appears highly sufficient. The extrapolation method was comparably accurate when used for the assessment of intraindividual changes in lung condition occurring between two successive CTs (Table 4). Thus, the extrapolation method also appears suitable for analysis of serial CT data, such as the measurement of hyperaeration or consolidation at different airway pressures or for assessing the evolution of a disease [4, 5, 8, 11, 16, 22, 23].

Reconstruction with intervals between consecutive sections has been widely used in qCT studies, but no particular interval could be proposed as an optimal standard [7, 31]. Thus, we tested whether reducing the number of CT sections analyzed to five or three, respectively, would allow extrapolation with comparable accuracy. Although bias values did not differ significantly between extrapolation from five versus ten CT sections, the limits of agreement were significantly broader for extrapolation from five CT sections. Extrapolation from only three CT sections significantly compromised the assessment of  $V_{\text{total}}$  and  $M_{\text{total}}$ .

**Table 4** Analysis of intraindividual changes

	Absolute changes between CTs	Bias for agreement of methods
$V_{\text{total}}$ (ml)	510 (28–2,309)	−0.4 (−89.4 to 90.3)
$V_{\text{non}}$ (%)	6 (0–36)	−0.2 (−0.9 to 0.4)
$V_{\text{poor}}$ (%)	9 (1–32)	−0.1 (−1.3 to 1.1)
$V_{\text{normal}}$ (%)	16 (0–59)	0.3 (−1.1 to 1.6)
$V_{\text{hyper}}$ (%)	3 (0–11)	0.0 (−0.6 to 0.6)
$M_{\text{total}}$ (g)	220 (22–1,672)	−13.1 (−55.5 to 29.3)
$M_{\text{non}}$ (%)	12 (0–55)	−0.4 (−2.0 to 1.3)
$M_{\text{poor}}$ (%)	8 (0–40)	−0.1 (−1.7 to 1.6)
$M_{\text{normal}}$ (%)	16 (2–74)	0.4 (−1.3 to 2.1)
$M_{\text{hyper}}$ (%)	1 (0–3)	0.0 (−0.2 to 0.2)
Gas content (%)	13 (1–46)	0.3 (−0.5 to 1.0)

The accuracy of the extrapolation method for the assessment of intraindividual changes between two successive CTs was tested in 26 patients. Absolute changes of parameters are given in the left column. Bias (95% limits of agreement) for the agreement of extrapolated changes and the corresponding values from all CT sections are shown in the right column. Data are median (range). All subvolumes and submasses were calculated as percentage of  $V_{\text{total}}$  or  $M_{\text{total}}$ , respectively

$V_{\text{total}}/M_{\text{total}}$  total lung volume or mass;  $V_{\text{non}}/M_{\text{non}}$  nonaerated volume or mass;  $V_{\text{poor}}/M_{\text{poor}}$  poorly aerated volume or mass;  $V_{\text{normal}}/M_{\text{normal}}$  normally aerated volume or mass;  $V_{\text{hyper}}/M_{\text{hyper}}$  hyperaerated volume or mass;  $V_{\text{gas}}$  pulmonary gas volume

Although the bias values for extrapolation of the relative subvolumes and submasses from three CT sections did not differ significantly from the bias values obtained for extrapolation using five or ten CT sections, the limits of agreement widened further (Table 3). It is obviously impossible to find a universally acceptable upper limit for the deviation from the values calculated from all CT sections. For the judgement of clinical acceptability, however, it may be helpful to infer from recent applications of qCT. Changes in qCT-derived parameters (e.g., nonaerated lung

tissue) in the magnitude of 5% were used either to stratify patients [4, 5] or to define a particular lung condition [15]. Because extrapolation from ten CT sections results in bias values close to zero and limits of agreement well below 5% it may be the best choice, especially when accurate analysis of absolute quantities such as  $V_{\text{total}}$  or  $M_{\text{total}}$  is required.

Image reconstruction had no influence on bias and limits of agreement (Table 2). This is important because the appropriateness of the assumption that lung boundaries are linear instead of curved is sensitive to thickness of and distance between CT sections. Moreover, reconstruction parameters can influence the apparent amount of especially hyperaerated lung regions, which needs to be considered when using the extrapolation methods in very thin sections reconstructed with an overenhancing filter [42].

Finally, neither the lung condition nor the distribution of infiltrates influenced the accuracy of the extrapolation. While CTs with diffuse, homogeneously distributed or gravity-dependent lung opacifications were not expected to be a challenge for the extrapolation method [21, 44], small, patchy infiltrates could be a problem. However, we did not find greater bias values in our subgroup of patients with patchy distributions (Table 1).

#### Limitations of our study

We validated the accuracy of the extrapolation method in a large number of CTs obtained in patients with a broad variety of lung conditions. However, prospective validation is lacking and the retrospective study design may have introduced potential confounders such as varying degrees of inspiration during CT. Consequently,  $V_{\text{total}}$  and  $V_{\text{gas}}$  as well as volumes and masses of differently aerated lung compartments reported here cannot be compared with previous studies. For our analysis, however, no particular degree of inspiration was required. In fact, as a result of the varying degree of inspiration, we could demonstrate the accuracy of the extrapolation method for a broad range of lung volumes.

The main difference between prospective and retrospective selection of CT sections would be the slice position, which may differ by a few millimeters. Real prospective evaluation of the extrapolation method would require exposing patients to increased radiation (i.e., one

helical scan plus ten slices), which we considered unjustified.

We have only evaluated the extrapolation method for 5- and 10-mm slice thickness. When, for example, only 1-mm sections are available, two problems need to be considered. Thicker sections limit spatial resolution and, consequently, larger amounts of hyperaeration have been measured in thin juxtadiaphragmatic CT sections [45]. However, thicker sections provide better density averaging and may thus be more representative of the regional mean density [42]. Also, the interval between 1-mm CT sections would be greater than the mean interval in our study. The use of thickened slabs (calculated from multiple 1-mm sections) for extrapolation could solve this problem [46], but requires validation.

Although we could not test it prospectively, we retrospectively demonstrated the accuracy of the extrapolation method for assessing intraindividual changes between repeat CTs. The range of changes observed between two successive CTs in our study is comparable to other reports [4], and we see no plausible reason which should preclude the use of the extrapolation method for serial CT measurements.

#### Conclusion

The extrapolation method evaluated in this work seems to be a promising approach to reduce radiation exposure of patients who undergo CT for the analysis of lung aeration, if used prospectively. It can also shorten the time required for the CT-based quantification of differently aerated lung compartments, total lung volume, and total lung mass especially in lungs with infiltrates. These advantages could make quantitative analysis of pulmonary CT more practicable and foster their implementation into research and clinical use. Future validation of our extrapolation method is warranted. Not only to test its applicability in research animals, but also to evaluate the usefulness of the extrapolation method for clinical applications such as the setting of PEEP.

**Acknowledgments** This work was supported by institutional funding.

#### References

1. Coxson HO, Mayo J, Lam S, Santyr G, Parraga G, Sin DD (2009) New and current clinical imaging techniques to study chronic obstructive pulmonary disease. *Am J Respir Crit Care Med* 180:588–597
2. Daly M, Miller PR, Carr JJ, Gayzik FS, Hoth JJ, Meredith JW, Stitzel JD (2008) Traumatic pulmonary pathology measured with computed tomography and a semiautomated analytic method. *Clin Imaging* 32:346–354
3. Gattinoni L, Caironi P, Pelosi P, Goodman LR (2001) What has computed tomography taught us about the acute respiratory distress syndrome? *Am J Respir Crit Care Med* 164:1701–1711

4. Gattinoni L, Caironi P, Cressoni M, Chiumello D, Ranieri VM, Quintel M, Russo S, Patroniti N, Cornejo R, Bugedo G (2006) Lung recruitment in patients with the acute respiratory distress syndrome. *N Engl J Med* 354:1775–1786
5. Caironi P, Cressoni M, Chiumello D, Ranieri M, Quintel M, Russo SG, Cornejo R, Bugedo G, Carlesso E, Russo R, Caspani L, Gattinoni L (2010) Lung opening and closing during ventilation of acute respiratory distress syndrome. *Am J Respir Crit Care Med* 181:578–586
6. Sumikawa H, Johkoh T, Yamamoto S, Takahei K, Ueguchi T, Ogata Y, Matsumoto M, Fujita Y, Natsag J, Inoue A, Tsubamoto M, Mihara N, Honda O, Tomiyama N, Hamada S, Nakamura H (2006) Quantitative analysis for computed tomography findings of various diffuse lung diseases using volume histogram analysis. *J Comput Assist Tomogr* 30:244–249
7. Madani A, Keyzer C, Gevenois PA (2004) Computed tomography assessment of lung structure and function in pulmonary emphysema. *Eur Respir Mon* 30:145–160
8. Perez A 4th, Coxson HO, Hogg JC, Gibson K, Thompson PF, Rogers RM (2005) Use of CT morphometry to detect changes in lung weight and gas volume. *Chest* 128:2471–2477
9. Washko GR, Martinez FJ, Hoffman EA, Loring SH, Estepar RS, Diaz A, Sciruba FC, Silverman EK, Han M, Decamp M, Reilly JJ, NETT Research Group (2010) Physiologic and computed tomographic predictors of outcome from lung volume reduction surgery. *Am J Respir Crit Care Med* 181:494–500
10. Patroniti N, Bellani G, Maggioni E, Manfio A, Marcora B, Pesenti A (2005) Measurement of pulmonary edema in patients with acute respiratory distress syndrome. *Crit Care Med* 33:2547–2554
11. Rouby JJ, Puybasset L, Nieszkowska A, Lu Q (2003) Acute respiratory distress syndrome: lessons from computed tomography of the whole lung. *Crit Care Med* 31(Suppl):S285–S295
12. Caironi P, Carlesso E, Gattinoni L (2006) Radiological imaging in acute lung injury and acute respiratory distress syndrome. *Semin Respir Crit Care Med* 27:404–415
13. Fernandez-Bustamante A, Easley RB, Fuld M, Mulreany D, Hoffman EA, Simon BA (2009) Regional aeration and perfusion distribution in a sheep model of endotoxemic acute lung injury characterized by functional computed tomography imaging. *Crit Care Med* 37:2402–2411
14. Malbouisson LM, Muller JC, Constantin JM, Lu Q, Puybasset L, Rouby JJ, CT Scan ARDS Study Group (2001) Computed tomography assessment of positive end-expiratory pressure-induced alveolar recruitment in patients with acute respiratory distress syndrome. *Am J Respir Crit Care Med* 163:1444–1450
15. Borges JB, Okamoto VN, Matos GF, Caramez MP, Arantes PR, Barros F, Souza CE, Victorino JA, Kacmarek RM, Barbas CS, Carvalho CR, Amato MB (2006) Reversibility of lung collapse and hypoxemia in early acute respiratory distress syndrome. *Am J Respir Crit Care Med* 174:268–278
16. Terragni PP, Rosboch G, Tealdi A, Corno E, Menaldo E, Davini O, Gandini G, Herrmann P, Mascia L, Quintel M, Slutsky AS, Gattinoni L, Ranieri VM (2007) Tidal hyperinflation during low tidal volume ventilation in acute respiratory distress syndrome. *Am J Respir Crit Care Med* 175:160–166
17. Grasso S, Stripoli T, Sacchi M, Trerotoli P, Staffieri F, Franchini D, De Monte V, Valentini V, Pugliese P, Crovace A, Driessen B, Fiore T (2009) Inhomogeneity of lung parenchyma during the open lung strategy: a computed tomography scan study. *Am J Respir Crit Care Med* 180:415–423
18. Chiumello D, Cressoni M, Polli F, Cozzi P, Lazzerini M, Raimondi N, Fumagalli R, Radrizzani D, Gattinoni L (2006) Is it possible to reduce the exposition to ionizing radiation for lung computed tomography scan analysis? *Crit Care* 10(Suppl 1):P9
19. Reske AW, Hepp P, Heine C, Schmidt K, Seiwerts M, Gottschaldt U, Reske AP (2007) Analysis of the nonaerated lung volume in combinations of single computed tomography sections—is extrapolation to the entire lung feasible? *Crit Care* 11(Suppl 2):P206
20. Lu Q, Malbouisson LM, Mourgeon E, Goldstein I, Coriat P, Rouby JJ (2001) Assessment of PEEP-induced reopening of collapsed lung regions in acute lung injury: are one or three CT sections representative of the entire lung? *Intensive Care Med* 27:1504–1510
21. Puybasset L, Cluzel P, Gusman P, Grenier P, Preteux F, Rouby JJ, CT Scan ARDS Study Group (2000) Regional distribution of gas and tissue in acute respiratory distress syndrome. I. Consequences for lung morphology. *Intensive Care Med* 26:857–869
22. Schreiter D, Reske A, Stichert B, Seiwerts M, Bohm SH, Kloeppel R, Josten C (2004) Alveolar recruitment in combination with sufficient positive end-expiratory pressure increases oxygenation and lung aeration in patients with severe chest trauma. *Crit Care Med* 32:968–975
23. Cornejo R, Diaz JC, Repetto C, Suarez P, Arellano D, Rouliez K, Diaz G, Romero C, Mezzano E, Riquelme AB, Ramos C (2009) Comparison of potentially recruitable lung (PRL) in supine versus prone position. Preliminary data. *Intensive Care Med* 35(Suppl 1):S126
24. Rylander C, Högman M, Perchiazzi G, Magnusson A, Hedenstierna G (2004) Oleic acid lung injury: a morphometric analysis using computed tomography. *Acta Anaesthesiol Scand* 48:1123–1129
25. Wrigge H, Zinslerling J, Neumann P, Muders T, Magnusson A, Putensen C, Hedenstierna G (2005) Spontaneous breathing with airway pressure release ventilation favors ventilation in dependent lung regions and counters cyclic alveolar collapse in oleic-acid-induced lung injury: a randomized controlled computed tomography trial. *Crit Care* 9:R780–R789
26. Simon BA (2000) Non-invasive imaging of regional lung function using X-ray computed tomography. *J Clin Monit* 16:433–442
27. Rylander C, Tylén U, Rossi-Norrlund R, Herrmann P, Quintel M, Bake B (2005) Uneven distribution of ventilation in acute respiratory distress syndrome. *Crit Care* 9:R165–R171
28. Reske AW, Gast HA, Seiwerts M, Kahn T, Gottschaldt U, Schreiter D, Josten C, Amato MBP, Reske AP (2009) Evaluation of a method to quicken the CT-based quantification of lung aeration for the entire lung. *Intensive Care Med* 35(Suppl 1):P302
29. Bland JM, Altman DG (1986) Statistical methods for assessing agreement between two methods of clinical measurement. *Lancet* 1(8476):307–310
30. Dewitte K, Fierens C, Stöckl D, Thienpont LM (2002) Application of the Bland–Altman plot for interpretation of method-comparison studies: a critical investigation of its practice. *Clin Chem* 48:799–801
31. Madani A, De Maertelaer V, Zanen J, Gevenois PA (2007) Pulmonary emphysema: radiation dose and section thickness at multidetector CT quantification—comparison with macroscopic and microscopic morphometry. *Radiology* 243:250–257



32. Zaporozhan J, Ley S, Weinheimer O, Eberhardt R, Tsakiris I, Noshi Y, Herth F, Kauczor HU (2006) Multi-detector CT of the chest: influence of dose onto quantitative evaluation of severe emphysema: a simulation study. *J Comput Assist Tomogr* 30:460–468
33. Sluimer I, Schilham A, Prokop M, van Ginneken B (2006) Computer analysis of computed tomography scans of the lung: a survey. *IEEE Trans Med Imaging* 25:385–405
34. Ley-Zaporozhan J, Ley S, Unterhinninghofen R, Weinheimer O, Saito Y, Kauczor HU, Szabo G (2008) Quantification of lung volume at different tidal volumes and positive end-expiratory pressures in a porcine model by using retrospective respiratory gated 4D-computed tomography. *Invest Radiol* 43:461–469
35. Markstaller K, Arnold M, Döbrich M, Heitmann K, Karmrodt J, Weiler N, Uthmann T, Eberle B, Thelen M, Kauczor HU (2001) A software tool for automatic image-based ventilation analysis using dynamic chest CT-scanning in healthy and in ARDS lungs. *Rofo* 173:830–835
36. David M, Karmrodt J, Bletz C, David S, Herweling A, Kauczor HU, Markstaller K (2005) Analysis of atelectasis, ventilated, and hyperinflated lung during mechanical ventilation by dynamic CT. *Chest* 128:3757–3770
37. Gattinoni L, Pelosi P, Vitale G, Pesenti A, D'Andrea L, Mascheroni D (1991) Body position changes redistribute lung computed-tomographic density in patients with acute respiratory failure. *Anesthesiology* 74:15–23
38. Gattinoni L, Pelosi P, Crotti S, Valenza F (1995) Effects of positive end-expiratory pressure on regional distribution of tidal volume and recruitment in adult respiratory distress syndrome. *Am J Respir Crit Care Med* 151:1807–1814
39. Zinslerling J, Wrigge H, Neumann P, Muders T, Magnusson A, Hedenstierna G, Putensen C (2005) Methodologic aspects of attenuation distributions from static and dynamic thoracic CT techniques in experimental acute lung injury. *Chest* 128:2963–2970
40. Gattinoni L, Pesenti A, Bombino M, Baglioni S, Rivolta M, Rossi F, Rossi G, Fumagalli R, Marcolin R, Mascheroni D, Torresin A (1988) Relationships between lung computed tomographic density, gas exchange, and PEEP in acute respiratory failure. *Anesthesiology* 69:824–832
41. Hedenstierna G, Strandberg A, Brismar B, Lundquist H, Svensson L, Tokics L (1985) Functional residual capacity, thoraco-abdominal dimensions and central blood volume during general anesthesia with muscle paralysis and mechanical ventilation. *Anesthesiology* 62:247–254
42. Reske AW, Busse H, Amato MB, Jaekel M, Kahn T, Schwarzkopf P, Schreiter D, Gottschaldt U, Seiwerts M (2008) Image reconstruction affects computer tomographic assessment of lung hyperinflation. *Intensive Care Med* 34:2044–2053
43. Stolk J, Dirksen A, van der Lugt AA, Hutsebaut J, Mathieu J, de Ree J, Reiber JH, Stoel BC (2001) Repeatability of lung density measurements with low-dose computed tomography in subjects with alpha-1-antitrypsin deficiency-associated emphysema. *Invest Radiol* 36:648–651
44. Borges JB, Janot GF, Okamoto VN, Caramez MP, Barros F, Souza CE, Carvalho CRR, Amato MBP (2003) Is there a true cephalocaudal lung gradient in ARDS? *Am J Respir Crit Care Med* 167(Suppl):A740
45. Vieira SR, Nieszowska A, Lu Q, Elman M, Sartorius A, Rouby JJ (2005) Low spatial resolution computed tomography underestimates lung overinflation resulting from positive pressure ventilation. *Crit Care Med* 33:741–749
46. Wedegärtner U, Yamamura J, Nagel HD, Aldefeld D, Brinkmann C, Popovych S, Buchert R, Weber C, Adam G (2007) Image quality of thickened slabs in multislice CT chest examinations: postprocessing vs direct reconstruction. *Rofo* 179:373–379